J Neurophysiol 109: 1250–1258, 2013.
First published December 12, 2012; doi:10.1152/jn.00533.2011.

Roles of default-mode network and supplementary motor area in human vigilance performance: evidence from real-time fMRI

Oliver Hinds,[1] Todd W. Thompson,[1] Satrajit Ghosh,[2] Julie J. Yoo,[1] Susan Whitfield-Gabrieli,[1,3] Christina Triantafyllou,[3] and John D. E. Gabrieli[1,3]

[1]*Department of Brain and Cognitive Sciences, Massachusetts Institute of Technology, Cambridge, Massachusetts;* [2]*Research Laboratory of Electronics, Massachusetts Institute of Technology, Cambridge, Massachusetts; and* [3]*A. A. Martinos Brain Imaging Center at the McGovern Institute for Brain Research, Massachusetts Institute of Technology, Cambridge, Massachusetts*

Submitted 30 June 2011; accepted in final form 7 December 2012

Hinds O, Thompson TW, Ghosh S, Yoo JJ, Whitfield-Gabrieli S, Triantafyllou C, Gabrieli JD. Roles of default-mode network and supplementary motor area in human vigilance performance: evidence from real-time fMRI. *J Neurophysiol* 109: 1250–1258, 2013. First published December 12, 2012; doi:10.1152/jn.00533.2011.—We used real-time functional magnetic resonance imaging (fMRI) to determine which regions of the human brain have a role in vigilance as measured by reaction time (RT) to variably timed stimuli. We first identified brain regions where activation before stimulus presentation predicted RT. Slower RT was preceded by greater activation in the default-mode network, including lateral parietal, precuneus, and medial prefrontal cortices; faster RT was preceded by greater activation in the supplementary motor area (SMA). We examined the roles of these brain regions in vigilance by triggering trials based on brain states defined by blood oxygenation level-dependent activation measured using real-time fMRI. When activation of relevant neural systems indicated either a good brain state (increased activation of SMA) or a bad brain state (increased activation of lateral parietal cortex and precuneus) for performance, a target was presented and RT was measured. RTs on trials triggered by a good brain state were significantly faster than RTs on trials triggered by a bad brain state. Thus human performance was controlled by monitoring brain states that indicated high or low vigilance. These findings identify neural systems that have a role in vigilance and provide direct evidence that the default-mode network has a role in human performance. The ability to control and enhance human behavior based on brain state may have broad implications.

fMRI; state; behavior; control; human; attention; parietal; motor cortex

HUMANS EXHIBIT ALTERNATING periods of enhanced and degraded behavioral performance (Verplank et al. 1952; Gilden et al. 1995), which can partly be attributed to fluctuations in vigilance or general alertness (Warm and Parasuraman 2007). The neural mechanisms of performance fluctuations are largely unknown, but one factor influencing performance may be the brain state that precedes action. Neuroimaging studies have found correlation between prestimulus brain activation and performance on subsequent trials (Fernández et al. 1999; Weissman et al. 2006; Fox et al. 2007; Boly et al. 2008; Leber et al. 2008), suggesting that the neural state before trial presentation influences performance. These findings raise the possibility that performance can be controlled by restricting trial presentation to times when the participant is most or least prepared to perform.

Address for reprint requests and other correspondence: O. Hinds, 77 Massachusetts Ave., 46-4033, Cambridge, MA 02139 (e-mail: ohinds@mit.edu).

We aimed to identify neural systems that underlie vigilance task performance. In two experiments, we measured vigilance as reaction time (RT) to a temporally sparse and unpredictable cue. In *experiment 1*, we used functional magnetic resonance imaging (fMRI) to measure precue blood oxygenation level-dependent (BOLD) activations correlated with faster or slower RT to a subsequent target to define anatomically specific brain states that may enhance or degrade vigilance. We hypothesized that greater activation in motor-task planning regions (those exhibiting premovement electrophysiological or neuroimaging activity) would be associated with enhanced vigilance and thus faster RT. One such region is supplementary motor area (SMA) (Deecke and Kornhuber 1978; Cunnington et al. 2002). We also hypothesized that greater activation in brain regions of the default-mode network, a network more active during rest than during performance (Raichle et al. 2001), would be associated with degraded vigilance. The default-mode network has been interpreted as mediating greater attention to internal thoughts relative to external percepts (Greicius et al. 2003; Weissman et al. 2006), although some studies argue that portions of the default-mode network mediate stimulus-dependent thought (Gilbert et al. 2006).

In *experiment 2*, we aimed to determine whether prestimulus activation in brain regions predictive of RT in *experiment 1* could be used to manipulate vigilance task performance. We asked whether we could control performance by presenting task cues only during brain states that were predicted to either facilitate or degrade performance. Target presentation was automatically triggered by brain states (activation in regions predictive of performance in *experiment 1*) measured continuously by real-time fMRI (rtfMRI). The key question was whether human performance could be controlled by presenting stimuli during brain states associated with superior relative to inferior performance.

Previous research has shown that BOLD magnitude in task-relevant areas predicts behavioral performance (Brewer et al. 1998; Wagner et al. 1998; Fernández et al. 1999; Ress et al. 2000). In addition, studies of brain regulation have shown that task performance can be affected (Rockstroh et al. 1990; Weiskopf et al. 2004; DeCharms et al. 2005; Caria et al. 2010). Our goal was to show that performance can be controlled by manipulating trial presentation based on a real-time monitoring of brain state.

The use of rtfMRI to enhance human performance has implications beyond this vigilance task. First, such a discovery

would open a new frontier for enhancing human performance through measurement of brain preparedness for optimal performance. Second, fMRI would become a method for manipulating human behavior based on activation, rather than merely correlating activation and behavior.

EXPERIMENT 1

Materials and Methods

Participants. Participants were healthy young adults who gave informed written consent as approved by the Massachusetts Institute of Technology human participants committee (COUHES). There were 15 participants (mean age: 26.3 yr; range: 21–34 yr; 6 females).

Vigilance task. Participants performed a classical vigilance task (Sturm et al. 1999) while in an MR scanner. The stimulus display consisted of a central fixation cross that transformed into a target (filled disk) upon trial presentation. Participants responded to the target by pressing a button with the right index finger (Fig. 1). Instructions were to stay alert and to respond to the target as quickly as possible. No performance feedback or indication of experimental condition was provided to the participant.

fMRI acquisition. All scans were performed using a 3T Trio MR System and a 32-channel, phased-array head coil (Siemens Healthcare, Erlangen, Germany). Structural scans were acquired using a three-dimensional T1-weighted MP-RAGE pulse sequence with a voxel size of $1 \times 1 \times 1$ mm^3, flip angle = 7°, echo time (TE) = 3.48 ms, inversion time (TI) = 1,100 ms, repitition time (TR) = 2,530 ms, and GRAPPA in the phase encode direction with an acceleration factor of 2. For functional scans, the BOLD signal was measured using a single shot gradient echo, echo-planar imaging (EPI) pulse sequence with imaging parameters: TR = 2,000 ms, TE = 30 ms, bandwidth = 2298 Hz, and flip angle = 90°. Thirty-two 3.5-mm thick slices (plus a 10% slice gap) were acquired during each TR with in-plane resolution = 3.125×3.125 mm^2.

The purpose of *experiment 1* was to identify brain regions in which activation before target presentation predicted RT and to do so in a rapid way so that these regions could be identified in each participant in *experiment 2* as regions of interest (ROIs) in a localizer for rtfMRI monitoring of brain states. In *experiment 1*, each participant underwent an initial functional localizer scan to locate ROIs in default-mode and motor planning and performance brain regions. The localizer task had three conditions: passive viewing of a fixation cross to locate default-mode regions, performance from memory of a simple

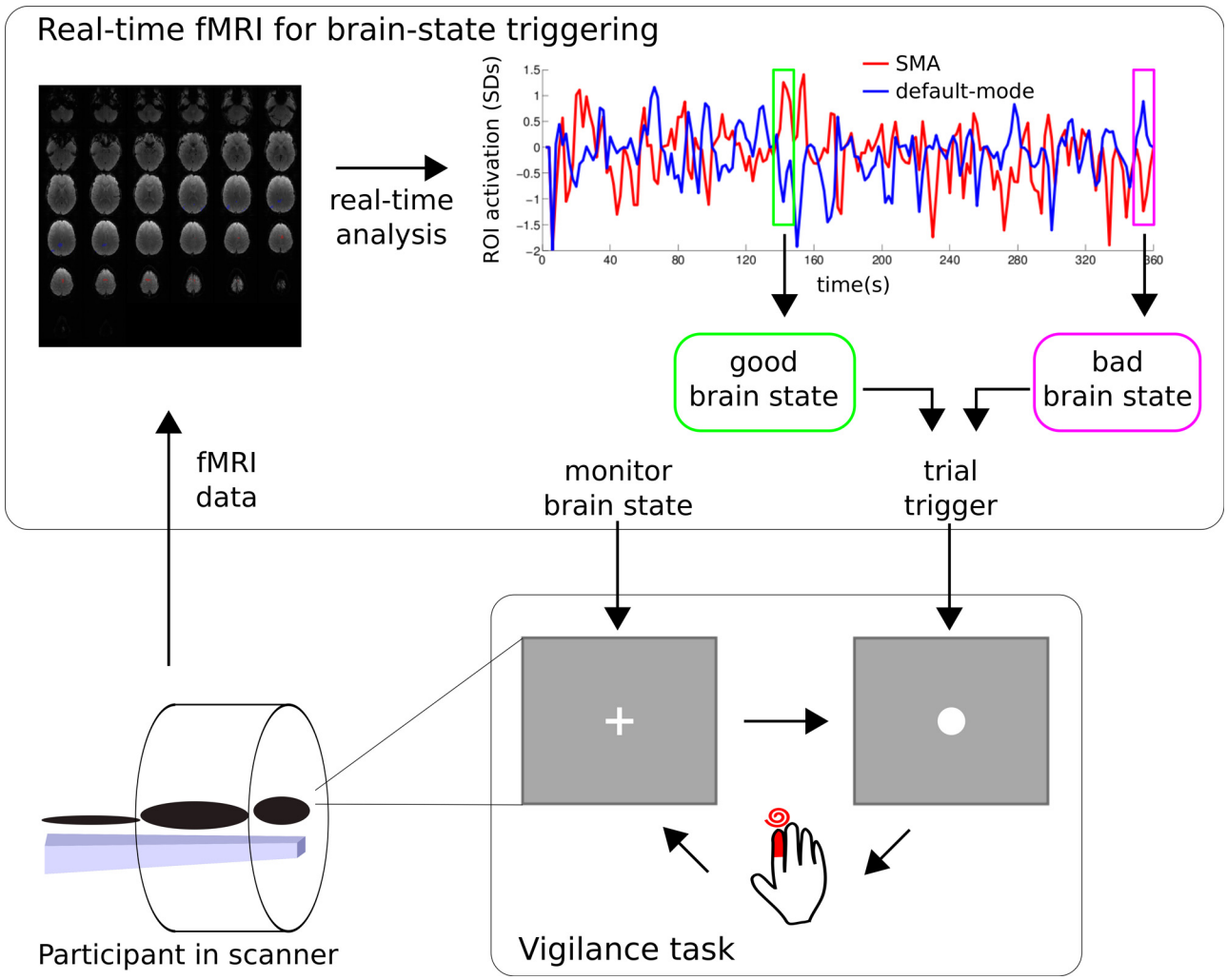

Fig. 1. Schematic demonstrating the vigilance task and brain-state triggering experimental process. During scans for the study to determine brain regions predictive of vigilance state, no real-time functional magnetic resonance imaging (fMRI) component was used, and the participant performed the vigilance task depicted at *bottom* with target appearance following a random schedule (between 16 and 26 s between trials). During scans for the study to control performance, vigilance brain state was monitored using real-time fMRI, as shown at *top*. If real-time fMRI analysis of supplementary motor area (SMA) and default-mode indicated a difference of >1SD for any measurement, a vigilance task trial was triggered (*top right*).

sequence of button presses (AABABBAAABBB) with the right index (A) and middle (B) fingers to locate motor planning and performance brain regions, and continuous tapping of the right index finger at a rate of about 1 Hz (data not used in this study). A complete cycle of the three conditions lasted 48 s (16 s for each block). Six block cycles were presented for a total imaging time of 4 min 48 s (144 measurements) for the functional localizer.

To image brain states predictive of vigilance performance, participants then underwent eight runs while performing the vigilance task. Vigilance trials were presented based on a predetermined stimulus schedule that was the same for every participant. There were between 16 and 26 s separating task trials, with the schedule randomized and balanced to cancel any consistent effect of lingering hemodynamic response from previous trials. Each vigilance task run lasted 5 min (150 measurements).

Defining default-mode and motor task-related ROIs. To define ROIs for individual participants, we first performed an fMRI analysis on the functional localizer. Preprocessing was accomplished using SPM5 (www.fil.ion.ucl.ac.uk/spm/). The localizer scan was motion corrected by alignment to the temporal mean of the time series. Each volume was then spatially smoothed via convolution with an isotropic Gaussian kernel of full-width at half-maximum of 6.25 mm in each dimension, and voxel timeseries were temporally demeaned and high pass filtered with a cutoff period of 96 s.

To determine the average magnitude of BOLD activation during the sequence condition of the localizer task, we fit a general linear model (GLM) to each voxel time course. The GLM design matrix included a column representing hypothesized BOLD activation, which was generated by convolving a boxcar timeseries constructed of ones during periods of motor sequence performance and zeros otherwise with an estimate of the hemodynamic impulse response function (sum of 2 Gamma functions). This column of interest was accompanied by design matrix columns to account for signal components of no interest to our experiment, such as participant head motion parameters, the mean intensity over the time course, the temporal derivative of the column of interest (included to account for slight deviations from the model hemodynamic response), and BOLD activation during the continuous finger tapping condition.

We examined motor control activation (sequence > fixation) and default activation (fixation > sequence) via *t*-tests in a set of predetermined motor performance-related and default-mode brain regions, respectively. Group-averaged ROI masks are shown in Fig. 2. ROIs for each region were chosen from individual participant *t* maps, which were initially thresholded at $t_{127} = 3.0$ ($P = 0.005$, uncorrected for the multiple ROIs tested), and then the threshold was increased until clusters of suprathreshold voxels separated between adjacent brain regions. This approach was necessary because we required a precisely defined ROI and there is substantial individual variation in BOLD activation strength among people. Although this process was observer dependent, in no case were subthreshold voxels included in an ROI. In each participant, we identified four ROIs more active during the sequence condition than during rest in motor control regions: primary motor cortex, SMA, and bilateral cerebellum. We also identified four ROIs less active during the sequence condition than during rest: left and right parietal lobes, medial prefrontal cortex (MPFC), and precuneus. SMA, MPFC, and precuneus ROIs were bilateral, spanning the interhemispheric fissure. Motor cortex ROIs were left-hemisphere only (all participants were right handed).

All vigilance task functional scans were motion corrected to the same target used for the functional localizer scan. Voxel time courses were extracted from each ROI mask and then high-pass filtered with a cutoff period of 104 s (run specific) and converted to percent signal change by subtracting the mean signal level over all collected time points within a particular voxel from each voxel time point, then dividing the result by the mean signal, and multiplying the result by 100. The spatial mean signal of these preprocessed voxel time courses was computed to yield a participant specific ROI time course over the eight runs of the vigilance experiment.

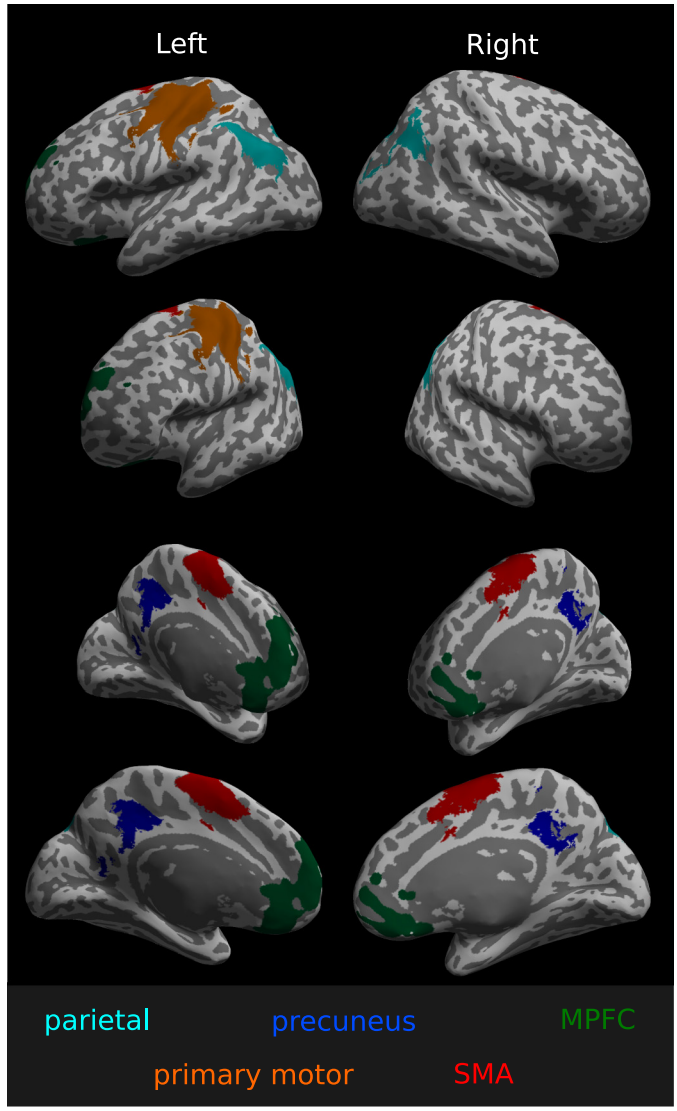

Fig. 2. *Experiment 1*: group-averaged region of interest (ROI) masks derived from the sequence condition of the functional localizer. ROIs were projected onto individual participant brain surfaces, which were registered to a surface template to determine the average ROIs.

Correlation between pretrial BOLD and RT. The correlation between RT and pretrial BOLD signal within each ROI for each participant was computed via linear regression for independent samples (custom analysis software implemented in MATLAB 7.5; Mathworks, Natick, MA). Linear regression is sensitive to outliers because a few extreme values can disproportionally affect regression model parameters. This is potentially problematic in the context of vigilance because trials with long (or absent) RTs may represent a fundamentally different brain state than other slower than average trials and could potentially dominate the regression. To minimize the influence of outlier trial RTs on BOLD/RT correlations, we estimated the probability density of the RT for each participant and derived an outlier threshold that separated trials where the participant had improbably long RT from "normal" responses. Local likelihood density estimation (Loader 1999) (bin width = 0.01 ms, h = 0.025 ms) was used to estimate the probability density function of RT for each participant. The RT outlier threshold was then computed by estimating the time separating the first (dominant) mode of the density from

later (secondary) modes by computing the derivative of the density and locating the first rising zero crossing using the same parameters used for estimating the density itself. Trials where RT exceeded this threshold (or were absent) were discarded. Over the whole group only 4.1 ± 3.9 (mean ± SD) trials were discarded.

For each participant, the time course of BOLD/RT correlations were computed at several lags relative to trial onset to produce a result similar to a peristimulus-time correlation diagram. Over individual lags of between four TRs before and eight TRs after trial presentation, ROI BOLD measurements at that lag were correlated with RT on the associated trial using linear regression. Pearson correlation coefficients r were converted into z-scores by $z = \log\sqrt{\frac{1+r}{1-r}}$. The mean BOLD/RT correlation across participants (within ROI) was tested for being different from zero using a one-tailed t-test based on direction of the functional localizer activation. The threshold was $P < 0.05$ for all analyses. In addition to the correlations between prestimulus activation and RT, we examined the effects sizes of the ROI correlations, temporal evolution of the BOLD signal, and BOLD/RT correlations in each ROI and whether the level of spontaneous BOLD signal just before trial presentation effected the degree of the evoked response.

Results

Significant positive correlations between prestimulus activation (measured 2 s before the task cue) and RT were observed in MPFC ($t_{14} = 2.20$; $P = 0.02$; $d = 0.57$), precuneus ($t_{14} = 2.49$; $P = 0.01$; $d = 0.64$), and left parietal ($t_{14} = 6.00$; $P = 0.00002$; $d = 1.55$) ROIs (Fig. 3) . The right parietal ROI also trended towards significance ($t_{14} = 1.21$; $P = 0.12$; $d = 0.31$). Prestimulus activation in SMA was significantly negatively correlated with RT ($t_{14} = -1.90$; $P = 0.04$; $d = 0.49$). Here, Cohen's d is a measure of effect size. No significant BOLD/RT correlation was observed for either primary motor or cerebellar ROIs.

To provide an additional sense of the effect size of RT correlation, the statistics of the percent of RT variance explained by ROI signals (r^2) was computed. For default-mode regions, the left parietal ROI explained 7.7 ± 2.6% of RT variance, the right parietal ROI explained 6.7 ± 3.0%, the precuneus ROI explained 4.2 ± 2.4%, and the MPFC ROI explained 8.6 ± 2.8%. For motor-related regions, the SMA ROI explained 12.1 ± 2.9% of RT variance, the primary motor ROI explained 2.5 ± 2.5%, the left cerebellum ROI explained 1.3 ± 2.4%, and the right cerebellum explained 1.7 ± 3.3%.

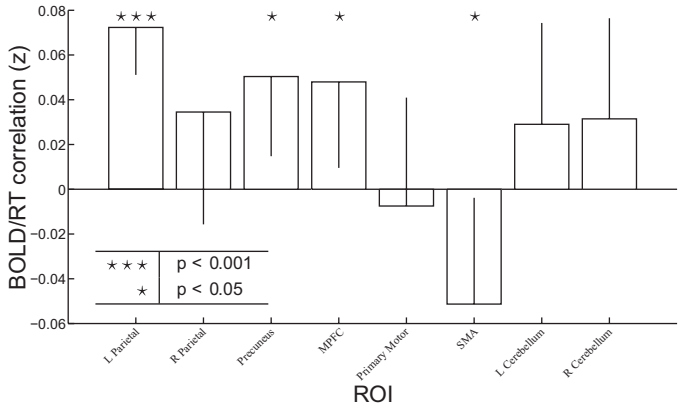

Fig. 3. *Experiment 1*: correlation of RT with pretrial blood oxygenation level-dependent (BOLD) signal within seven ROIs defined via an independent functional localizer scan. Error bars represent 95% confidence intervals and extend in the direction appropriate for the one-tailed test. Pretrial activation was measured 2 s [1 repetition time (TR)] before the task cue. Different symbols indicate false positive probabilities determined via a one-tailed t-test respecting the direction of ROI activation in the functional localizer task.

We also probed the temporal evolution of both mean BOLD signal and BOLD/RT correlation within each ROI for between 8 s before 16 s after trial presentation (Fig. 4). The temporal progression of mean BOLD signal indicated that all motor regions, but none of the default-mode regions, exhibited substantial evoked response to the trial. BOLD/RT correlation peaked in the SMA before the peak mean BOLD signal associated with the trial, whereas BOLD/RT correlations in primary motor cortex and cerebellar regions peaked at about the same time as the mean BOLD signal. Task deactivated regions generally show positive BOLD/RT correlations before the trial but no BOLD/RT correlations in response to the trial itself.

We used the temporal progression of BOLD to ask whether the level of spontaneous BOLD signal just before trial presentation effected the degree of the evoked response. To this end, we correlated the BOLD signal from each ROI measured 2 s before trial presentation with the ROI signal measured 6 s after trial presentation (TRs-1 and -3 in Fig. 4). We found significant negative correlations between spontaneous and evoked BOLD in the left parietal ROI ($P = 0.01$; $r^2 = 0.40$), the precuneus ROI ($P = 0.0002$; $r^2 = 0.66$), and the SMA ROI ($P = 0.004$; $r^2 = 0.49$). Correlations were also negative, but not significant, for the right parietal ROI ($P = 0.3$; $r^2 = 0.08$), the MPFC ROI ($P = 0.08$; $r^2 = 0.21$), the primary motor ROI ($P = 0.1$; $r^2 = 0.16$), or either left ($P = 0.3$; $r^2 = 0.09$) or right ($P = 0.3$; $r^2 = 0.07$) cerebellar ROIs.

EXPERIMENT 2

Materials and Methods

Participants. Participants were healthy young adults who gave informed written consent as approved by the Massachusetts Institute of Technology human participants committee (COUHES). There were 15 participants (mean age: 23.0 yr; range: 19–30 yr; 9 females).

fMRI acquisition. The purpose of *experiment 2* was to determine whether RT performance could be controlled by presenting stimuli when activation was high or low in brain regions from *experiment 1* that were associated with slow RTs (default-mode regions) or fast RTs (SMA). In an initial scan to identify ROIs for subsequent real-time analysis, participants performed the same motor sequence functional localizer task used in *experiment 1*. After image reconstruction and online motion correction on the scanner computer system, each functional volume was sent via a TCP/IP connection using a custom data sender created with help from Siemens Healthcare to a dedicated fMRI data analysis computer, where it was stored. The fMRI acquisition parameters and vigilance task in *experiment 2* were identical to those used in *experiment 1*.

Online ROI definition. As soon as the functional localizer scan was completed, an fMRI analysis using FMRIB Software Library (FSL: http://www.fmrib.ox.ac.uk/fsl/) was performed on the EPI volumes to delineate SMA and default-mode ROIs. Images were preprocessed via smoothing with an isotropic Gaussian kernel of full-width at half maximum of 6.25 mm, four-dimensional intensity normalization and high-pass filtering with a cutoff of 96 s.

The localizer stimulus schedule was used to construct a GLM design matrix consisting of bases representing hypothesized activation to each of the tapping conditions and their temporal derivatives. Analysis proceeded via an initial least-squares fit of the GLM to each voxel time course to derive an estimate of temporal autocorrelations, which were accounted for by prewhitening using FSL default approach. A final GLM fit was performed on the resulting data and the parameter estimates were transformed into statistical images representing activation in the sequence tapping task condition.

The SMA ROI was defined by thresholding the motor sequence > rest statistic volume at an initial value of $t_{127} = 3.0$; ($P = 0.005$, uncorrected for multiple comparisons) and choosing the cluster of

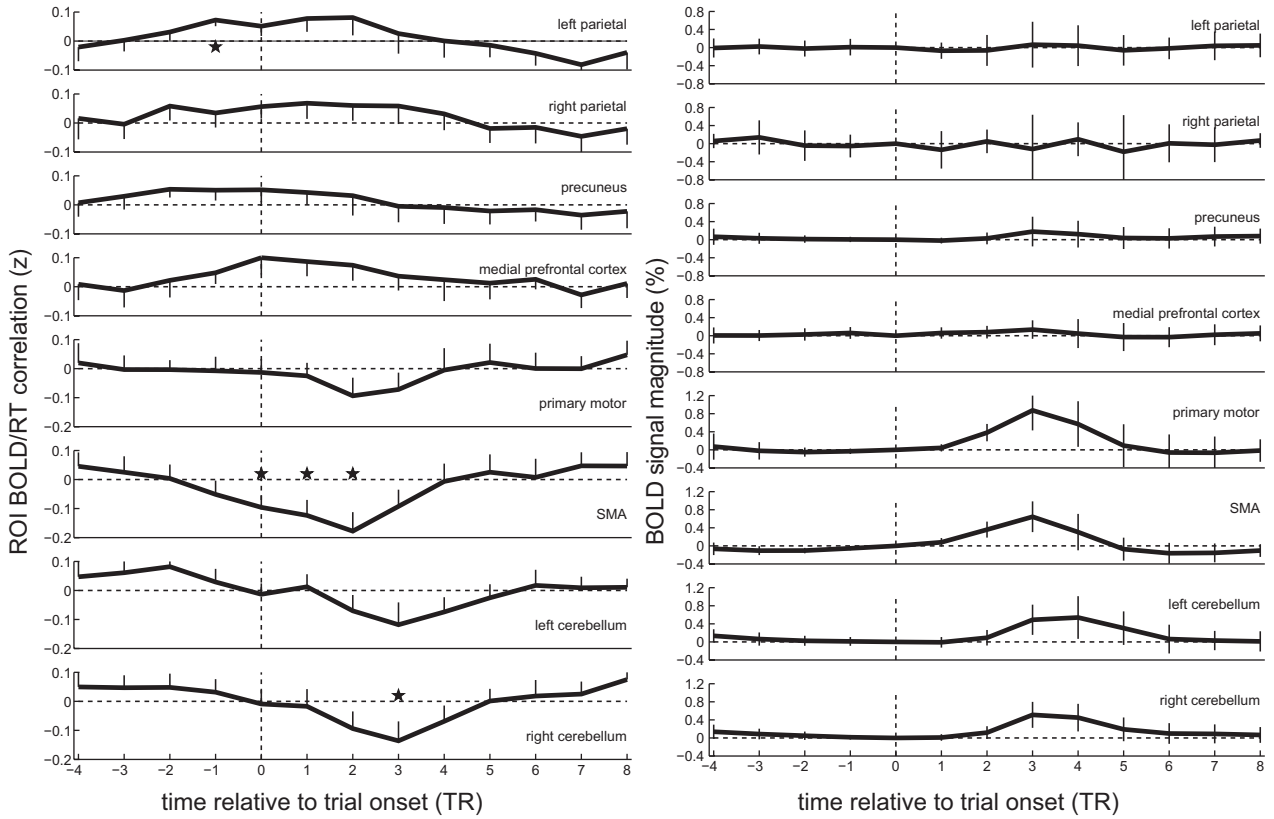

Fig. 4. *Experiment 1*: temporal progression of BOLD/RT correlation (*left*) and mean ROI BOLD %signal change (*right*) relative to trial onset in the vigilance task. Error bars for BOLD/RT correlation (*left*) represent the 95% confidence interval for the one-tailed *t*-test based on the direction of ROI activation in the independent functional localizer scan. Stars indicate a significant difference from zero after correction for comparison of multiple time points. Error bars for BOLD % signal change (*right*) are presented for reference only, and represent 99.9% confidence intervals for a two-tailed *t*-test after correcting the temporal progression of each participant to the value at the time of trial onset.

above threshold voxels on the midline near the border of the frontal and parietal lobes. Default-mode ROIs were defined by thresholding the rest > motor sequence statistic volume and choosing three clusters: one in the precuneus on the midline near the border of the parietal and occipital lobes, and one each in the right and left parietal cortex. The three separate default-mode ROIs were combined and treated as a single ROI during the rtfMRI analysis. MPFC was not included in the default-mode ROI for real-time use because this brain region exhibits substantial BOLD signal artifacts related to its proximity to the sinuses and mouth. Commonly, these artifacts are accounted for during data analysis post hoc, which is not possible in real time.

To visualize the group ROIs, we used spatial normalization available as part of the SPM5 software package to spatially warp the mean functional image of the localizer scan into Montreal Neurological Institute (MNI) space. The resulting transformation was applied to the SMA and default-mode ROIs for each participant, resulting in ROIs in MNI space. The ROIs were then averaged across participants to create a map of the average location of SMA and default-mode ROIs. For visualization, this map was projected onto a surface representation of the cortex generated automatically by the FREESURFER software package (http://surfer.nmr.mgh.harvard.edu/) from a single participant structural MRI scan (in MNI space) available as part of the MRICRON software package (http://www.sph.sc.edu/comd/rorden). The SMA and default-mode ROI masks that were used to define brain state are shown (averaged over participants on a group average surface) in Fig. 5.

Controlling performance based on brain state. Participants underwent eight brain-state triggering fMRI scans, each lasting 6 min, while BOLD fluctuations were measured using rtfMRI analysis as described in Hinds et al. (2010). During triggering, functional runs of incoming images from the scanner were analyzed to estimate activation levels in the SMA and default-mode ROIs. To accomplish this, we performed a voxelwise incremental GLM fit where the design matrix included bases to account for the mean voxel signal and linear trends. Also,

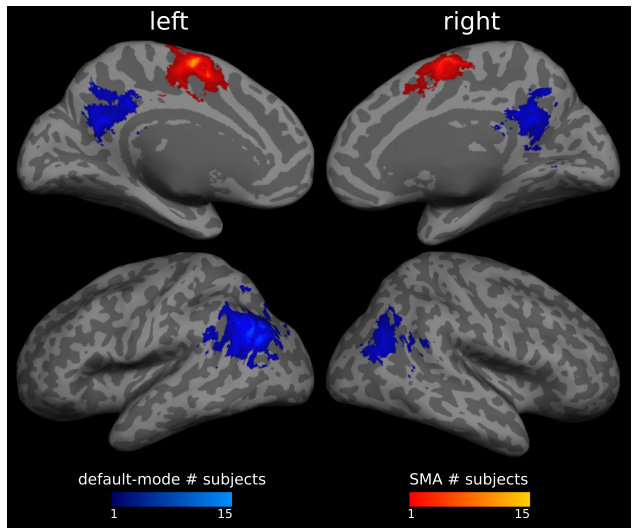

Fig. 5. *Experiment 2*: regions that defined brain state. Group SMA (red) and default-mode (blue) ROIs after spatial normalization, group averaging, and projection onto a cortical surface in Montreal Neurological Institute (MNI) space. Mean MNI coordinates of the ROIs were SMA: [−0.7, −2.2, 59.5], precuneus: [−0.4, −50.1, 31.3], left parietal: [−43.6, −64.3, 33.2], and right parietal [48.4, −63.8, 27.3].

additional GLM bases were added in real time to account for the evoked hemodynamic response related to vigilance task trials.

To discount components of the voxel signal due to nuisance sources (e.g., low-frequency signal drifts), the GLM reconstruction of the expected voxel intensity at time t was subtracted from the measured voxel intensity at time t, leaving a residual signal that has components due to two sources: BOLD signal fluctuations and unmodeled fMRI noise. This residual was scaled by an estimate of voxel reliability, which was computed as the average GLM residual over the first 20 functional images, during which time no task trials were presented. This analysis results in an estimate of the strength of activation at each voxel at time t in units of standard deviation (SD).

Activations in SMA and default-mode ROIs were computed as the median SD of the voxels in each ROI. Brain state was defined as the difference between SMA and default-mode ROI activations, with a good brain state defined by SMA activation greater than default-mode activation by at least 1SD and a bad brain state defined by default-mode activation greater than SMA activation by at least 1SD. On detection of a brain state predictive of performance (good or a bad), a vigilance task 12 trials was triggered. To accomplish this, a signal was sent to the stimulus computer via a TCP/IP connection, where the stimulus program received this signal and triggered a trial presentation, to which RT was measured. To allow the BOLD response resulting from a triggered target to return to baseline, no triggers were possible during a 20-s window following a triggered trial. The time delay between collection of a complete EPI volume and trial trigger was <0.5 s. A schematic depicting the brain state monitoring and trial triggering process is shown in Fig. 1.

Performance analysis. We assessed whether performance was successfully controlled by examining the difference in speed of performance between trials triggered by good vs. bad brain states. To evaluate behavioral control over the group, the mean RT difference for each participant was entered into a t-test to determine whether good state RT was faster than bad state RT. We computed the behavioral difference between RT on trials triggered in good vs. bad brain state by first computing the within run difference between mean RT in each condition and then computing the mean difference across runs. We chose this approach because *1*) the rtfMRI analysis treats each run separately and therefore splitting the behavioral data into runs accounts for potential differences in trigger criteria among them (e.g., due to run-specific noise factors), and *2*) participant performance varies over the course of the experiment and comparing behavioral data collected nearby in time factors out global performance variations.

This approach of computing behavioral difference in RT between conditions has the potential drawback that runs with relatively few trials will be weighted identically to runs with many trials. To determine if this was an issue, we computed the total number of trials in each run for each participant and then computed the coefficient of variation of number of trials in a run over the eight runs. The number of trials in each run was remarkably consistent within participant, with a mean (±SD) coefficient of variation of just 0.13 (±0.06).

We hypothesized that RTs on trials triggered by greater activation in default than SMA regions would be significantly slower than RTs on trials triggered by greater activation in SMA than default regions ($P < .05$, paired t-test). We also performed additional analyses to compare results from *experiments 1* and *2*, and to verify that findings were not secondary to other factors, such as outlier behavioral values, sizes of individual ROIs, and ordering of good-state or bad-state trials, and that ROIs were similar, on average, across *experiments 1* and *2*.

Results

Mean vigilance task RT was significantly faster for trials triggered by good brain states than by bad brain states: the means (±SE) difference in RT was 22 ± 11 ms ($t_{14} = -2.05$; $P = 0.03$; $d = 0.51$, one-tailed, paired t-test; Fig. 6). Good-state trials were also significantly faster than bad-state trials if overall means were analyzed independent of runs ($t_{14} = -2.07$; $P = 0.029$) or after regressing out RT-interstimulus interval via standard linear regression ($W_+ = 24$; $P = 0.021$). Among participants, 73% (11/15) exhibited faster mean RT in good vs. bad brain state. On average, there were 46 ± 2.1 good and 41 ± 1.9 (mean ± SE) bad trials per participant over the whole experiment. There were 11.2 ± 0.85 trials per run, and the average interstimulus interval was 32.3 ± 2.5 s.

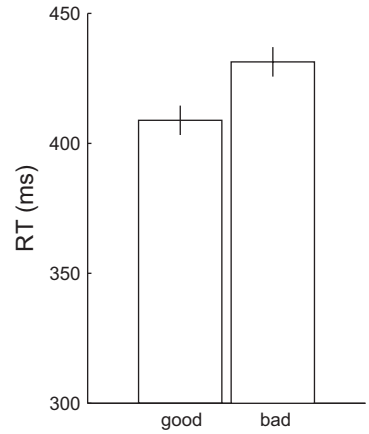

Fig. 6. *Experiment 2*: group average reaction time (RT) data when trials were triggered by detection of a good or bad brain state. RT was significantly faster for good than bad brain state trials (signed-rank test for good RT < bad RT: $t_{14} = 2.05$; $P = 0.03$). Error bars represent 95% confidence intervals computed considering the within participants nature of these comparisons (Cousineau 2005).

A post hoc analysis on the data collected in *experiment 2* was performed using the same methods used for *experiment 1*. The progression of brain state relative to trial presentation was computed for both good and bad brain states separately (Fig. 7*A*). Good and bad brain states are significantly different only at the time of trial presentation ($P < 0.05$, after correction for the 10 time points tested). The progression of the SMA and default-mode ROI signals were also computed for both good and bad trials (Fig. 7*B*). The default-mode ROI drives good brain states, while both ROIs contribute strongly to bad brain states.

To address the possibility that outlier participants drove the observed RT differences, we performed a post hoc analysis leaving out the three participants who exhibited mean RT differences >1SD from the mean difference (>19.2 ms or <64.6 ms). After outlier participant exclusion, the good brain state RT was still significantly faster than bad brain state RT ($t_{11} = 2.5$; $P = 0.015$), indicating that outlier behavioral performance was not influencing the outcome.

The sizes of the ROIs used to trigger trials varied across individuals, but there was no significant relation between the size of any ROI and either mean RT difference or mean overall RT for any of the brain regions that were used for brain state monitoring ($P > 0.1$ for each region). Also, there was no significant difference between the number of good and bad trials over participants ($t_{14} = 1.72$; $P = 0.11$), no correlation between the balance of good and bad trials and RT difference between conditions ($r^2 = 0.002$; $P = 0.87$), no temporal trend in RT across the experimental session ($t_{14} = 0.98$; $P = 0.34$), and no relationship between interstimulus interval and RT ($t_{14} = 0.78$; $P = 0.45$).

An analysis of the asymmetry of the interstimulus interval between good and bad conditions (performed identically to the analysis of RT differences between conditions) revealed no significant difference between the interval preceding good and bad trials (mean within run difference ± SD = 0.3 ± 2.7s; $t_{14} = 0.38$; $P = 0.71$). The mean ± SD interstimulus interval preceding was 33.6 ± 3.6 s for good trials and 31.0 ± 2.0 s for bad trials.

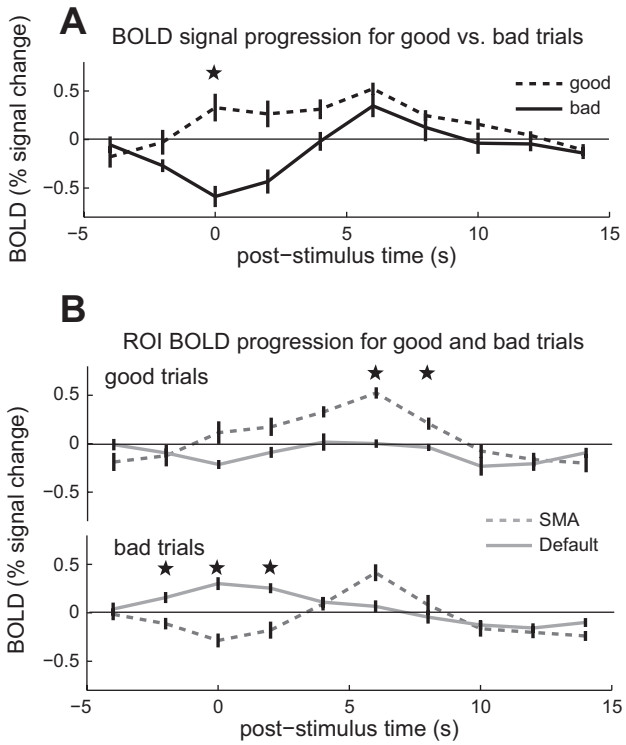

Fig. 7. *Experiment 2*: *A*: peristimulus-time diagram showing the progression of brain state (SMA minus default-mode ROI BOLD signal) relative to trial presentation separated by trial type. Good trial brain state (dashed line) and bad trial brain state (solid line) are significantly different from one another only at the trigger time. A substantial evoked response to the trial peaks at 6 s after trial presentation for both good and bad trials. *B*: peristimulus-time diagram of the SMA and default-mode ROI signals for good trials (*top*) and bad trials (*bottom*). In both *A* and *B*, stars represent significant differences between the dashed and solid lines after correction for comparison over the 10 time points.

We verified that the ROIs used in *experiment 1*, which were defined after the scanning, matched those used in *experiment 2*, which had to be defined instantly during the scanning session. Group-normalized parietal, precuneus, and SMA ROIs that were used to determine predictive brain state in *experiment 1* were plotted on an inflated representation of the cortical surface, and related to the ROIs used to measure brain state in *experiment 2*. Qualitatively, there was a high degree of similarity in the ROIs (Fig. 8).

DISCUSSION

We found evidence for brain states in brain regions that modulate vigilance task performance as measured by RT to sparse and unpredictable visual targets. In *experiment 1*, greater activation in SMA and lesser activation in multiple default-mode regions (MPFC, precuneus, and lateral parietal) predicted superior vigilance. In *experiment 2*, the roles of activation in SMA and precuneus and lateral parietal regions were determined by evidence that vigilance performance could be controlled by triggering trials based on ongoing brain states. These findings help define neural systems important for vigilance and also show that rtfMRI can be used to monitor brain states and alter human performance.

Brain Activation and Performance Fluctuations

This study relates separate lines of evidence for low-frequency fluctuations in task performance (Gilden et al. 1995) and low-frequency fluctuations in regional BOLD signal (Fox et al. 2005). Our results demonstrate that these fluctuations are related for vigilance, while prior studies have shown relations of such fluctuations to human performance. Variability in button press force correlated with BOLD fluctuations in primary motor cortex across two TRs after trial presentation (Fox et al. 2007). We observed a similar effect in SMA, but correlation between RT and SMA BOLD was observed sooner and over a longer period, from between one TR before to three TRs after trial presentation. Our findings that BOLD magnitude and RT correlations peaked after stimulus presentation in primary motor cortex are similar to the timing of the correlation between primary motor cortex and button press force (Fox et al. 2007). BOLD in cerebellar ROIs significantly correlated with RT two and three TRs after trial presentation. Prestimulus default-mode activation has also been associated with slower RT (or "lapses of attention") on a complex cognitive task (Weissman et al. 2006).

There is debate regarding the degree to which BOLD fluctuations reflect fluctuations in neural activity. Generally, studies using "resting state" fMRI (Biswal et al. 1995; Greicius et al. 2003; Fox et al. 2005) assume that low-frequency BOLD fluctuations reflect fluctuations in the activity level of neural populations. However, fluctuations in the BOLD signal could instead be attributable to the low-pass characteristics of the hemodynamic response to neural activity (Smith et al. 2008). A primate study using simultaneous fMRI and electrophysiology reported that resting BOLD fluctuations were closely linked to neural processes (Shmuel and Leopold 2008). These findings, however, were subsequently interpreted as fluctuations evoked by unintended stimuli (Logothetis et al. 2009). Whereas these primate studies found strong empirical relations between neural and BOLD fluctuations, another primate study reported that under periodic stimulus conditions the relationship between neural activity and the BOLD signal breaks down (Sirotin and Das 2008). Thus, even with invasive neural recordings in primates, the precise relations between BOLD fluctuations and neural activity remain difficult to characterize.

The present findings, however, provide strong evidence that low-frequency BOLD fluctuations reflect neural and psychological processes. Not only did the BOLD fluctuations in SMA

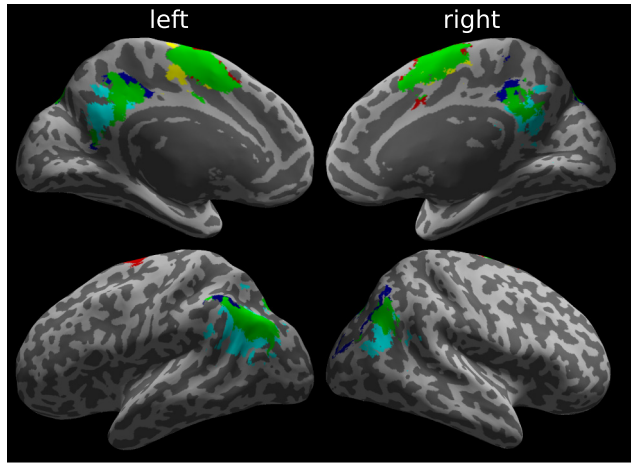

Fig. 8. Agreement between the parietal, precuneus, and SMA ROIs used in *experiment 1* and the default-mode and SMA ROIs used in *experiment 2*. Group-normalized and surface-projected ROIs for *experiment 1* are shown in red (SMA) and blue (parietal and precuneus) and for *experiment 2* in yellow (SMA) and cyan (default-mode). Regions of overlap are indicated in green.

and default-mode regions correlate with RT (*experiment 1*) but also those fluctuations could be used with rtfMRI to control vigilance task performance (*experiment 2*). There may well be circumstances where BOLD fluctuations do not reflect neural activity, but BOLD fluctuations in *experiment 2* could only be related to performance if they reflected neural activity and the mental processes mediated by that activity. An interesting question that will be left as future work is the relationship between the BOLD fluctuations we harnessed and the fluctuations that are commonly observed at rest.

Neuroanatomy of Vigilance in the Human Brain: SMA and Default-Mode Network

The present study provided support for SMA and the posterior (parietal and precuneus) components of the default-mode network as important components of the vigilance system. In *experiment 1*, SMA was the only motor region in which prestimulus activation correlated with faster RT, and the role of prestimulus activation for faster RT was demonstrated in *experiment 2*. Such a prestimulus role for SMA is consistent with electrophysiological and neuroimaging evidence about the role of SMA in motor planning (Tanji 1994). Electrophysiology studies in primates have found SMA neurons that fire preceding externally cued movements [reviewed in Nachev et al. (2008)]. In humans, electrical activity in SMA increases leading up to the execution of self-initiated movements [the Bereitschafts potential (Deecke and Kornhuber 1978)]. Neuroimaging studies have also revealed activation in SMA before externally cued movements such as those used in the present study (Jahanshahi et al. 1995; Cunnington et al. 2002). Prestimulus warnings that decrease RT activate pre-SMA (Yanaka et al. 2010). Activation in the present study included both the pre-SMA and SMA proper, so we are unable to relate our findings to distinctions between pre-SMA and SMA. SMA is associated with midbrain and thalamic circuits implicated in attention and vigilance (Sturm and Willmes 2001), but we did not observe a predictive effect in any subcortical region.

In the present study, participants could not predict exactly when a stimulus would appear, but over time on a given trial it is likely that they increasingly anticipated stimulus arrival. This may have induced a Bereitschafts potential, which we detected using rtfMRI, by presenting a target to allow completion of this quasi-internally generated movement. Alternatively, the SMA signal we measured could be unrelated to the Bereitschafts potential and simply indicate the degree of preparedness to respond to the cue in the absence of intentionality.

Experiment 2 provides evidence that activation in the default-mode network can be used to manipulate human behavior. There is interest in understanding the function of the default-mode network, but such an understanding has relied on indirect measures because activation occurs in the absence of behavior; indeed the default-mode network is defined by brain regions showing greater activation during rest than during active performance. Two kinds of indirect evidence have supported the hypothesis that the default-mode network mediates introspection rather than attention to the external environment (Raichle et al. 2001; Greicius et al. 2003). First, active tasks requiring introspection activate components of the default-mode network (Gusnard et al. 2001). The limitation of such studies is that performing a task dictates that the default-mode network is not in a default state. A second argument comes from studies showing that default-mode activation has been associated with easier tasks (McKiernan et al. 2003), worse memory formation (Daselaar et al. 2004), attention lapses (Weissman et al. 2006), more frequent mind wandering (Mason et al. 2007), and worse working memory performance (Whitfield-Gabrieli et al. 2009). In these studies, the behaviors measured were thought to be mediated by other brain regions that mediate attention, memory, or skill learning, rather than the default-mode network. Indeed, the ambiguity in interpreting psychological functions of the default-mode network due to absence of direct behavioral measurement is evident in an alternative interpretation of these data: that default-mode regions mediate stimulus-dependent thought rather than stimulus-independent thought (Gilbert et al. 2006). Specifically, MPFC and posterior cingulate were associated stimulus-dependent task conditions.

The results of *experiment 2*, however, argue that the default-mode network is associated with stimulus-independent thought, because triggering stimulus presentation via activation in the default-mode network resulted in slower RTs (e.g., worse stimulus-dependent performance). This is evidence that activation in the default-mode network is anticorrelated with the efficiency of simple RT. We did not include MPFC in *experiment 2* for concerns about the ability to measure real-time BOLD in the region, but greater prestimulus activation in MPFC correlated with slower RTs in *experiment 1*, and low-frequency fluctuations during rest are highly correlated in the default-mode network (Fox et al. 2005), so it is likely that the fluctuations that drove stimulus presentation in *experiment 2* from the precuneus and parietal regions were highly correlated with MPFC activations. Therefore, although it appears that there are conditions during which default-mode activation may be associated with stimulus-dependent thought (Gilbert et al. 2006), the present findings provide direct evidence that default-mode activation is associated with worse stimulus-dependent performance in the simplest behavioral case.

Controlling Human Performance

Controlling performance by monitoring brain states in specific neural systems has potential applications in behavior intervention and for testing neuroscientific hypotheses. The ability to objectively measure specific brain states makes enhancement of performance or learning by presenting information during optimal brain states possible. Learning has been enhanced in animals by triggering trials via invasively measured theta activity (Seager et al. 2002; Griffin et al. 2004). Here we show that network-specific activation reflecting brain states can be measured by rtfMRI and used to control performance noninvasively. Detection of brain states signaling potential subsequent performance errors can be used to remind the participant to maintain vigilance, to modify task demands online, to assess the reliability of behavioral responses, or to halt tasks altogether. Practical application of such knowledge will demand translation of this method to more portable technologies. Performance control via brain state monitoring may also have practical applications for testing novel neuroscientific hypotheses. Although fMRI is commonly used as a method for correlating BOLD with behavior, brain state-triggering transforms fMRI into a method for manipulating behav-

ior. Such a use of fMRI may provide a new method for characterizing the functions of regions in the human brain.

DISCLOSURES

No conflicts of interest, financial or otherwise, are declared by the author(s).

REFERENCES

Biswal B, Yetkin F, Haughton V, Hyde J. Functional connectivity in the motor cortex of resting human brain using echo-planar. *Magn Reson Med* 34: 537, 1995.

Boly M, Phillips C, Balteau E, Schnakers C, Degueldre C, Moonen G, Luxen A, Peigneux P, Faymonville M, Maquet P, Laureys S. Consciousness and cerebral baseline activity fluctuations. *Hum Brain Map* 29: 868–874, 2008.

Brewer J, Zhao Z, Desmond J, Glover G, Gabrieli J. Making memories: brain activity that predicts how well visual experience will be remembered. *Science* 281: 1185, 1998.

Caria A, Sitaram R, Veit R, Begliomini C, Birbaumer N. Volitional control of anterior insula activity modulates the response to aversive stimuli. A real-time functional magnetic resonance imaging study. *Biol Psychiatr* 68: 425–432, 2010.

Cousineau D. Confidence intervals in within-subject designs: a simpler solution to Loftus and Masson's method. *Tutorial Quant Methods Psych* 1: 42–45, 2005.

Cunnington R, Windischberger C, Deecke L, Moser E. The preparation and execution of self-initiated and externally-triggered movement: a study of event-related fMRI. *Neuroimage* 15: 373–385, 2002.

Daselaar S, Prince S, Cabeza R. When less means more: deactivations during encoding that predict subsequent memory. *Neuroimage* 23: 921–927, 2004.

DeCharms R, Maeda F, Glover G, Ludlow D, Pauly J, Soneji D, Gabrieli J, Mackey, S. Control over brain activation and pain learned by using real-time functional MRI. *Proc Natl Acad Sci USA* 102: 18626–18631, 2005.

Deecke L, Kornhuber H. An electrical sign of participation of the mesial supplementary motor cortex in human voluntary finger movement. *Brain Res* 159: 473–476, 1978.

Fernández G, Brewer J, Zhao Z, Glover G, Gabrieli D. Level of sustained entorhinal activity at study correlates with subsequent cued-recall performance: a fMRI study with high acquisition rate. *Hippocampus* 9: 35–44, 1999.

Fox M, Snyder A, Vincent J, Corbetta M, Van Essen D, Raichle M. The human brain is intrinsically organized into dynamic, anticorrelated functional networks. *Proc Natl Acad Sci USA* 102: 9673–9678, 2005.

Fox M, Snyder A, Vincent J, Raichle M. Intrinsic fluctuations within cortical systems account for intertrial variability in human behavior. *Neuron* 56: 171–184, 2007.

Gilbert S, Simons J, Frith C, Burgess P. Performance-related activity in medial rostral prefrontal cortex (area 10) during low-demand tasks. *J Exp Psychol* 32: 45–58, 2006.

Gilden D, Thornton T, Mallon M. 1/f noise in human cognition. *Science* 267: 1837–1839, 1995.

Greicius M, Krasnow B, Reiss A, Menon V. Functional connectivity in the resting brain: a network analysis of the default mode hypothesis. *Proc Natl Acad Sci USA* 100: 253–258, 2003.

Griffin A, Asaka Y, Darling R, Berry S. Theta-contingent trial presentation accelerates learning rate and enhances hippocampal plasticity during trace eyeblink conditioning. *Behav Neurosci* 118: 403- 411, 2004.

Gusnard D, Akbudak E, Shulman G, Raichle M. Medial prefrontal cortex and self-referential mental activity: relation to a default mode of brain function. *Proc Natl Acad Sci USA* 98: 4259–4264, 2001.

Hinds O, Ghosh S, Thompson TW, Yoo JJ, Whitfield-Gabrieli S, Triantafyllou C, Gabrieli JD. Computing moment to moment bold activation for real-time neurofeedback. *Neuroimage* 54: 361–368, 2011.

Jahanshahi M, Jenkins I, Brown R, Marsden C, Passingham R, Brooks D. Self-initiated versus externally triggered movements: I. An investigation using measurement of regional cerebral blood flow with PET and movement-related potentials in normal and parkinson's disease subjects. *Brain* 118: 913–933, 1995.

Leber A, Turk-Browne N, Chun M. Neural predictors of moment-to-moment fluctuations in cognitive flexibility. *Proc Natl Acad Sci USA* 105: 13592–13597, 2008.

Loader C. *Local Regression and Likelihood*. New York: Springer, 1999.

Logothetis, NK, Murayama, Y, Augath, M, Steffen, T, Werner, J, Oeltermann A. How not to study spontaneous activity. *Neuroimage* 45: 1080–1089, 2009.

Mason M, Norton M, Van Horn J, Wegner D, Grafton S, Macrae C. Wandering minds: the default network and stimulus-independent thought. *Science* 315: 393–395, 2007.

McKiernan K, Kaufman J, Kucera-Thompson J, Binder J. A parametric manipulation of factors affecting task-induced deactivation in functional neuroimaging. *J Cogn Neurosci* 15: 394–408, 2003.

Nachev P, Kennard C, Husain M. Functional role of the supplementary and pre-supplementary motor areas. *Nat Rev Neurosci* 9: 856–869, 2008.

Raichle M, MacLeod A, Snyder A, Powers W, Gusnard D, Shulman G. A default mode of brain function. *Proc Natl Acad Sci USA* 98: 676–682, 2001.

Ress D, Backus B, Heeger D. Activity in primary visual cortex predicts performance in a visual detection task. *Nature Neurosci* 3: 940–945, 2000.

Rockstroh B, Elbert T, Birbaumer N, Lutzenberger W. Biofeedback-produced hemispheric asymmetry of slow cortical potentials and its behavioural effects. *Int J Psychophysiol* 9: 151–165, 1990.

Seager M, Johnson L, Chabot E, Asaka Y, Berry S. Oscillatory brain states and learning: impact of hippocampal theta-contingent training. *Proc Natl Acad Sci USA* 99: 1616–1620, 2002.

Shmuel A, Leopold D. Neuronal correlates of spontaneous fluctuations in fMRI signals in monkey visual cortex: implications for functional connectivity at rest. *Hum Brain Map* 29: 751–761, 2008.

Sirotin Y, Das A. Anticipatory haemodynamic signals in sensory cortex not predicted by local neuronal activity. *Nature* 457: 475–479, 2008.

Smith S, Niazy R, Beckmann C, Miller K. Resting state networks-neither low frequency nor anticorrelated? *Neuroimage* 41, *Suppl* 1: S181–S227, 2008.

Sturm W, de Simone A, Krause BJ, Specht K, Hesselmann V, Radermacher I, Herzog H, Tellmann L, Muller-Gartner HW, Willmes K. Functional anatomy of intrinsic alertness: evidence for a frontoparietal-thalamic-brainstem network in the right hemisphere. *Neuropsychologia* 37: 797–805, 1999.

Sturm W, Willmes K. On the functional neuroanatomy of intrinsic and phasic alertness. *NeuroImage* 14: 76–84, 2001.

Tanji J. The supplementary motor area in the cerebral cortex. *Neurosci Res* 19: 251–268, 1994.

Verplank W, Collier G, Cotton J. Nonindependence of successive responses in measurements of the visual threshold. *Exp Psychol* 44: 273–282, 1952.

Wagner A, Schacter D, Rotte M, Koutstaal W, Maril A, Dale A, Rosen B, Buckner R. Building memories: remembering, and forgetting of verbal experiences as predicted by brain activity. *Science* 281: 1188–1191, 1998.

Warm J, Parasuraman R. Cerebral hemodynamics and vigilance. In: *Neuroergonomics: The Brain at Work*, edited by Parasuraman R, Rizzo M. Oxford, UK: Oxford Univ. Press, 2007, p. 147–158.

Weiskopf N, Scharnowski F, Veit R, Goebel R, Birbaumer N, Mathiak K Self-regulation of local brain activity using real-time functional magnetic resonance imaging (fMRI). *J Physiol* 98: 357–373, 2004.

Weissman D, Roberts K, Visscher K, Woldorff M. The neural bases of momentary lapses in attention. *Nat Neurosci* 9: 971–978, 2006.

Whitfield-Gabrieli S, Thermenos H, Milanovic S, Tsuang M, Faraone S, McCarley R, Shenton M, Green A, Nieto-Castanon A, LaViolette P. Hyperactivity and hyperconnectivity of the default network in schizophrenia and in first-degree relatives of persons with schizophrenia. *Proc Natl Acad Sci USA* 106: 1279–1284, 2009.

Yanaka H, Saito D, Uchiyama Y, Sadato N. Neural substrates of phasic alertness: a functional magnetic resonance imaging study. *Neurosci Res* 68: 51–58, 2010.